

## Article

# Synthesis Characterization and Highly Protective Efficiency of Tetraglycidyoxy Pentanal Epoxy Prepolymer as a Potential Corrosion Inhibitor for Mild Steel in 1 M HCl Medium

Rachid Hsissou <sup>1,\*</sup>, Redouane Lachhab <sup>2</sup>, Anouar El Magri <sup>3,\*</sup>, Siham Echihi <sup>4</sup>, Hamid Reza Vanaei <sup>5,\*</sup>,  
Mouhsine Galai <sup>2</sup>, Mohamed Ebn Touhami <sup>2</sup> and Mohamed Rafik <sup>1</sup>

- <sup>1</sup> Laboratory of Organic Chemistry, Catalysis and Environment, Department of Chemistry, Faculty of Sciences, Ibn Tofail University, BP 242, Kenitra 14000, Morocco; lrafik@yahoo.com
- <sup>2</sup> Laboratory of Advanced Materials and Process Engineering, Faculty of Sciences, Ibn Tofail University, BP 242, Kenitra 14000, Morocco; lachhabred1@gmail.com (R.L.); galaimouhsine@gmail.com (M.G.); mohamed.ebntouhami@uit.ac.ma (M.E.T.)
- <sup>3</sup> Euromed Polytechnic School, Euromed Research Center, Euromed University of Fes, Route de Meknès (Rond point Bensouda), Fès 30000, Morocco
- <sup>4</sup> Laboratory of Materials Engineering for the Environment and Natural Resources, Faculty of Sciences and Techniques, University Moulay Ismail of Meknes, BP 509 Boutalamine, Errachidia 52000, Morocco; echihisiham@gmail.com
- <sup>5</sup> Arts et Métiers Institute of Technology, CNAM, LIFSE, HESAM University, F-75013 Paris, France
- \* Correspondence: r.hsissou@gmail.com (R.H.); a.elmagri@ueuromed.org (A.E.M.); hamidreza.vanaei@ensam.eu (H.R.V.)



**Citation:** Hsissou, R.; Lachhab, R.; El Magri, A.; Echihi, S.; Vanaei, H.R.; Galai, M.; Ebn Touhami, M.; Rafik, M. Synthesis Characterization and Highly Protective Efficiency of Tetraglycidyoxy Pentanal Epoxy Prepolymer as a Potential Corrosion Inhibitor for Mild Steel in 1 M HCl Medium. *Polymers* **2022**, *14*, 3100. <https://doi.org/10.3390/polym14153100>

Academic Editors: Dapeng Wang and Guillermo Ahumada

Received: 21 June 2022

Accepted: 28 July 2022

Published: 30 July 2022

**Publisher's Note:** MDPI stays neutral with regard to jurisdictional claims in published maps and institutional affiliations.



**Copyright:** © 2022 by the authors. Licensee MDPI, Basel, Switzerland. This article is an open access article distributed under the terms and conditions of the Creative Commons Attribution (CC BY) license (<https://creativecommons.org/licenses/by/4.0/>).

**Abstract:** Anticorrosive protection efficiency of novel tetrafunctional epoxy prepolymer, namely 2,3,4,5-tetraglycidyoxy pentanal (TGP), for mild steel in 1 M HCl medium was assessed through potentiodynamic polarization (PDP), electrochemical impedance spectroscopy (EIS), scanning electron microscope (SEM), energy dispersive X-ray spectroscopy (EDS), contact angle (CA), adsorption isotherm model, temperature effect and thermodynamic parameters. The synthesized TGP was characterized and confirmed by Fourier transform infrared (FTIR) spectroscopy and nuclear magnetic resonance (NMR). The inhibitory efficiencies found at lower concentration of the prepolymer TGP were 85% (PDP) and 87.17% (EIS). PDP measurement illustrated that the TGP behaved as a mixed-type inhibitor in the realized solution. SEM and EDS analysis showed a significant decrease in the corrosion of the MS surface in the presence of the inhibitory prepolymer compared with the blank (1 M HCl). Langmuir adsorption isotherm is the most acceptable model to describe the TGP epoxy prepolymer on the MS area.

**Keywords:** synthesis; epoxy prepolymer TGP; FTIR/NMR characterization; anticorrosive protection; PDP/EIS measurements; SEM/EDS/CA analyses; Langmuir adsorption

## 1. Introduction

Mild steel surfaces are widely employed and investigated in large civil engineering projects because of their advantages of availability and excellent tensile and mechanical strength [1,2]. The introduction of organic inhibitors such as quinoxaline, quinoline, polymer composites and epoxy prepolymers has become one of the most effective approaches for retarding the corrosion of mild steel in different aggressive solutions [3–5]. Multifunctional epoxy prepolymer molecules possessing oxygen, sulfur and nitrogen heteroatoms and electronegative polar groups, as well as aldehydes, carboxyl, amino, oxirane groups have been used to display excellent protective abilities as corrosion inhibitors by forming a chemical bond with the metallic surface [6–9]. Epoxy prepolymer molecules have  $\pi$ -electrons and unsaturated donating and are able to accept electrons in their low-energy empty orbitals [10,11]. Epoxy prepolymer compounds have been investigated as excellent

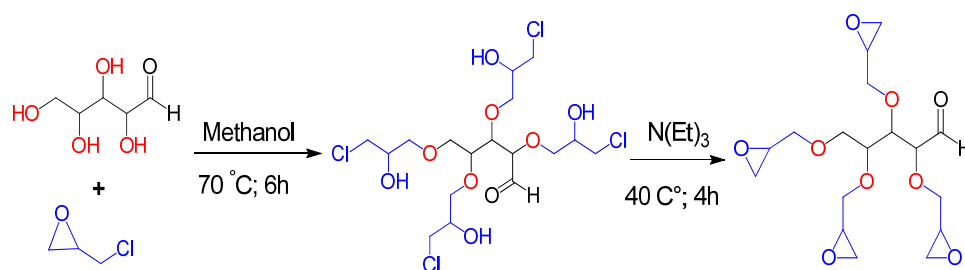
corrosion inhibitors because of their ability to adsorb readily to a metallic surface [12–14]. This class of epoxy prepolymer molecules has been investigated as corrosion inhibitors because of its synthesis by the condensation reaction of epichlorohydrin with compounds having mobile hydrogen in the presence of sodium hydroxide (NaOH) as the basis [15–17]. The presence of an oxirane group, carbonyl compounds and oxygen heteroatoms enables it to cooperate with an iron surface, facilitating the adsorption of epoxy prepolymer on the metallic area and acting as a corrosion inhibitor [18–21]. Damej et al. studied *N,N*-1-tri(oxiran-2-ylmethoxy)-5-((oxiran-2-ylmethoxy)thio)-1*H*-1,2,4-triazole-3-amine as a potential corrosion inhibitor for steel in 1 M HCl solution and found a high inhibitory efficiency of 92% at lower concentration (1 mM) [6].

In this work, the novel tetrafunctional epoxy prepolymer, namely, 2,3,4,5-tetraglycidyloxy pentanal (TGP), was synthesized by the condensation reaction of arabinose with epichlorohydrin in the presence of triethylamine as the basis. The synthesized TGP was characterized and confirmed by Fourier transform infrared (FTIR) spectroscopy and nuclear magnetic resonance (NMR). Additionally, TGP was used and investigated as a potential corrosion inhibitor for mild steel in 1 M HCl solution by potentiodynamic polarization technique, electrochemical impedance spectroscopy measurements, scanning electron microscope (SEM) analysis, energy dispersive X-ray spectroscopy (EDS) study and contact angle (CA) technique [22]. The last two decades have witnessed great progress in the prediction of the properties and chemical reactivity of different materials, despite their complexities, due to the development and advancement of numerical simulation systems. In addition, the adsorption isotherm model, temperature effect and thermodynamic parameters were investigated and thoroughly discussed [23–25].

## 2. Materials and Methods

### 2.1. Synthesis of 2,3,4,5-Tetraglycidyloxy Pentanal (TGP)

All chemical products used in this experimental section, such as arabinose (99%), epichlorohydrin (99%), methanol (99%) and triethylamine (99.5%), were purchased from Sigma Aldrich, Germany. All chemical products were employed without other purification. Novel tetrafunctional epoxy prepolymer, namely, 2,3,4,5-tetraglycidyloxy pentanal (TGP), was elaborated and developed by condensation reaction in two steps according to the procedure reported in the literature [15,16,26,27]. In a balloon of 100 mL fitted with refrigerant,  $4.73 \times 10^{-3}$  mol of the arabinose was dissociated in the methanol as solvent after we added  $2.42 \times 10^{-2}$  mol of epichlorohydrin under magnetic stirring at 70 °C for 6 h (Scheme 1). Additionally, we condensed  $2.54 \times 10^{-2}$  mol of triethylamine as the basis for the reaction mixture under magnetic stirring at 40 °C for 4 h (Scheme 1). Furthermore, methanol and triethylamine excess was removed with a rotary evaporator. Finally, we obtained a prepolymer of a brown color.



**Scheme 1.** Synthesis of TGP epoxy prepolymer.

### 2.2. Tested Material

The chemical composition of mild steel (MS) substrates used in the experimental section were C(14.55%), Si(0.68%), S(0.41%), Cr(15.64%), Mn(1.94%), Fe(57.99%), Ni(7.92%) and Mo(0.86%). The treatment of the MS electrode used has been widely reported in the literature [1,2,22].

### 2.3. Characterization Techniques

All functional groups of novel tetrafunctional epoxy prepolymer, namely, the 2,3,4,5-tetraglycidyoxy pentanal (TGP) synthesized, were identified and characterized by Fourier transform infrared (FTIR) and nuclear magnetic resonance (NMR), respectively. FTIR spectra were obtained with a Bruker AVANCE (300 MHz) spectrometer at room temperature. The light beam passed through the 5 mg sample. The analysis was carried out between 4000 and 400  $\text{cm}^{-1}$ , which corresponds to the energy range of the vibration of chemical bonds of organic molecules. Furthermore, NMR spectrometry was performed using a Bruker AVANCE (300 MHz) apparatus. The sample was dissolved in deuterated DMSO (DMSO- $d_6$ ), and the chemical shifts were expressed in ppm. Additionally, the MS electrode area plunged in 1 M HCl medium, both unprotected and protected with a lower concentration of TGP ( $10^{-3}$  M), was investigated by the scanning electron microscope (SEM) technique, energy dispersive X-ray (EDS) analysis and contact angle (CA) measurements. The SEM analysis was studied to make images of the MS electrode, both unprotected and protected with  $10^{-3}$  M of TGP, using a JEOL-JSM-5500 microscope Type. Then, EDS was used to determine the elemental chemical composition. The conditions of the measurement were as follows: the acceleration voltage was 15.00 kV, the magnification was  $\times 3500$ , the live time was 30.00 s, the real time was 31.97 s, the dead time was 6.00% and the count rate was 19,403.00 CPS. In addition, the electrochemical study was carried out in a three-electrodes cell using a Potentiostat/Galvanostat/SP-200 biological apparatus. The work electrode was mild steel (MS), the counter electrode was platinum (Pt) and the reference electrode was a saturated calomel electrode (SCE). Open circuit potential (OCP) was realized for 30 min for each assay after reaching the equilibrium state. The EIS study was carried out at OCP at a frequency range from 100 KHz to 10 mHz with 10 mV of signal amplitude. In addition, potentiodynamic polarization (PDP) was measured at 0.2 mV/s during potential range from  $-900$  to  $-0.1$  mV. Furthermore, the inhibition efficiencies for potentiodynamic polarization  $\eta_{\text{PDP}}$  and electrochemical impedance spectroscopy  $\eta_{\text{EIS}}$  were determined according to Equations (1) and (2):

$$\eta_{\text{PDP}} (\%) = \frac{i_{\text{corr}}^0 - i_{\text{corr}}}{i_{\text{corr}}^0} \times 100 \quad (1)$$

$$\eta_{\text{EIS}} (\%) = \frac{R_{\text{ct}} - R_{\text{ct}}^0}{R_{\text{ct}}} \times 100 \quad (2)$$

$R_{\text{ct}}^0$ ,  $R_{\text{ct}}$ ,  $i_{\text{corr}}^0$  and  $i_{\text{corr}}$  represent the charge transfer resistance unprotected, charge transfer resistance protected with varying concentrations of TGP, unprotected corrosion current densities and protected corrosion current densities with different concentrations of TGP, respectively.

## 3. Results

### 3.1. FTIR Characterization

The novel tetrafunctional epoxy prepolymer, namely, the 2,3,4,5-tetraglycidyoxy pentanal (TGP) synthesized, was recorded by utilizing Fourier transform infrared (FTIR) spectroscopy (BRUKER type) to determine and characterize the varying functional groups. The FTIR spectrum analysis of TGP is illustrated in Figure 1.

The absorption band in the FTIR spectrum of TGP appeared at  $3324 \text{ cm}^{-1}$ , which is attributed to the stretching vibrations of hydroxyl function (-OH) of an unclosed epoxy group [15]. The absorption band situated at  $2973 \text{ cm}^{-1}$  corresponds to aliphatic methylene ( $\text{CH}_2$ ) [15,16]. Furthermore, the absorption band assigned at  $2845 \text{ cm}^{-1}$  corresponds to C-H of aldehyde function [16]. Then, the absorption band located at  $1738 \text{ cm}^{-1}$  corresponds to aldehyde function (C=O) [27]. Additionally, the absorption bands at  $1432$ ,  $1396$  and  $1366 \text{ cm}^{-1}$  correspond to the stretching vibrations of aliphatic C-H [28]. Furthermore, the absorption bands which appeared at  $1090$ ,  $1050$  and  $1005 \text{ cm}^{-1}$  can be assigned to the asymmetric stretching vibration of C-O-C aliphatic ether function [15]. In addition, the

presence of the epoxy group is displayed by the characteristic absorption bands at 902 and 853  $\text{cm}^{-1}$ , which are attributed to stretching of C-O-C and C-O of oxirane group [15,27].

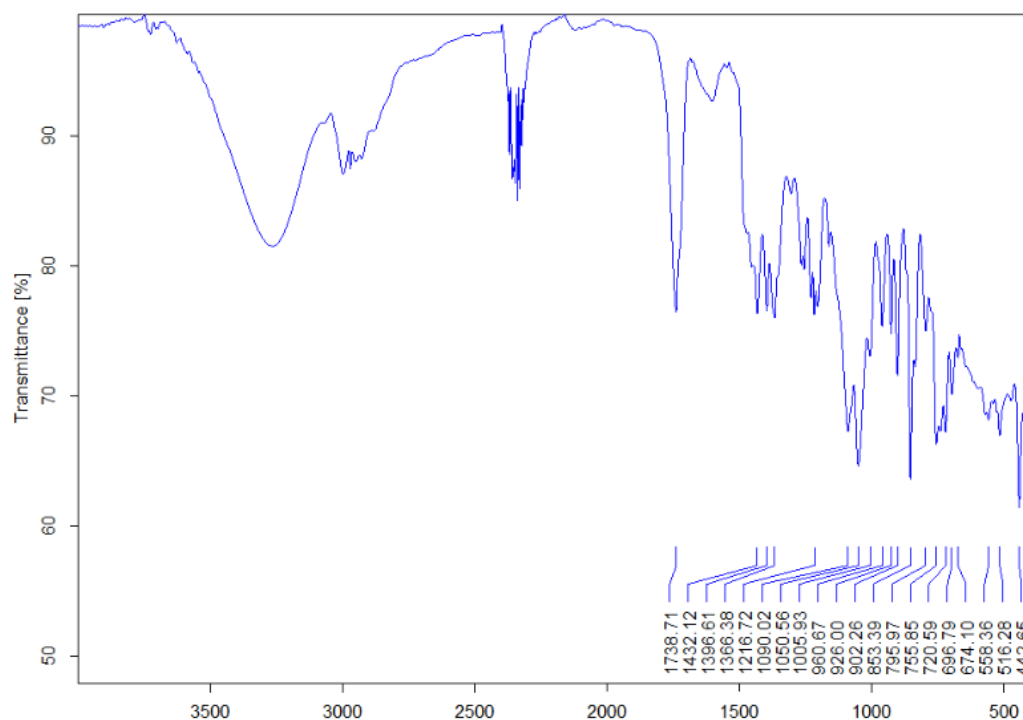


**Figure 1.** IR spectrum of synthesized TGP.

### 3.2. NMR Characterization

The synthesized 2,3,4,5-tetraglycidyloxy pentanal (TGP) was characterized and confirmed using  $^{13}\text{C}$  NMR spectroscopy to determine the carbon atoms. The NMR spectrum of TGP is illustrated in Figure 2.

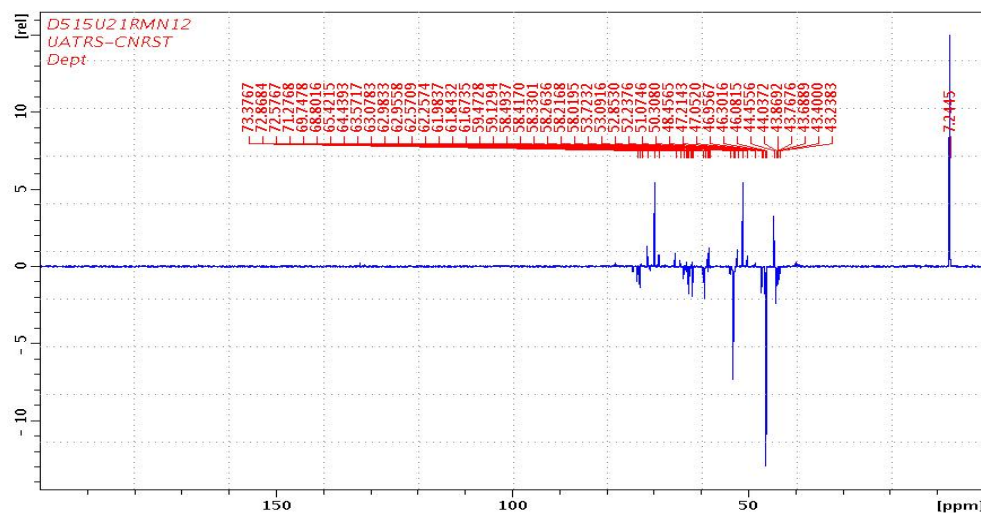


**Figure 2.** NMR spectrum of TGP synthesized.

The attribution of varying chemical shifts of the synthesized epoxy prepolymer is as follows:

$^{13}\text{C}$  RMN (ppm): 47 (s,  $\text{CH}_2$  of oxirane group), 52 (s, CH of oxirane group), 55 (s,  $\text{CH}_2$  related to oxirane and  $\text{O}-\text{CH}_2$ ) and 72 (s,  $\text{CH}_2$  linked to O and aliphatic CH).

### 3.3. PDP Analysis

To know and understand the kinetics of the electrochemical reactions occurring at the active centers of the MS electrode surface, both unprotected and protected by varying concentrations of the studied epoxy prepolymer in 1 M HCl solution at 298 K, potentiodynamic polarization curves were used and investigated as shown in Figure 3 and Table 1. The results illustrated in Table 1 show that the corrosion current density ( $i_{corr}$ ) diminished from  $983.0 \mu\text{A cm}^{-2}$  for unprotected to  $147.42 \mu\text{A cm}^{-2}$  for protected within the highest concentration of studied epoxy prepolymer ( $10^{-3} \text{ M}$ ) [3,29]. Additionally, within the lowest concentration ( $10^{-6} \text{ M}$ ), the inhibitory efficiency reached a value of 76.88% and gradually increased within the highest concentration ( $10^{-3} \text{ M}$ ) of the TGP epoxy prepolymer, reaching a highest value of 85.0% [16]. These results showed that the TGP epoxy prepolymer at low concentration could form a protective layer on the MS area by reducing the number of active centers and be used and investigated as a good inhibitor. Furthermore, in this experimental part, the difference between the potential ( $\Delta E_{corr}$ ) of the unprotected and protected with varying concentrations of TGP (from 21 to 45 mV) was less than 85 mV, showing that the investigated epoxy prepolymer acts as a mixed-type inhibitor [30,31]. These results revealed that the TGP epoxy prepolymer was able to stop substrate electrode dissolution at the anode as well as hydrogen gas evolution at the cathode. According to the data displayed in Table 1, careful analysis of the anodic and cathodic Tafel slopes suggests that, with the addition of the TGP prepolymer, both slopes were changed compared to the 1 M HCl solution alone [32]. Additionally, the reaction mechanisms, both anodic and cathodic, for the unprotected and protected by different concentrations of the epoxy prepolymer were confirmed to be constant as the shape of the polarization curves remained the same, showing that the epoxy prepolymer synthesized adsorbed on the metallic area through blocking the active centers [6,20].

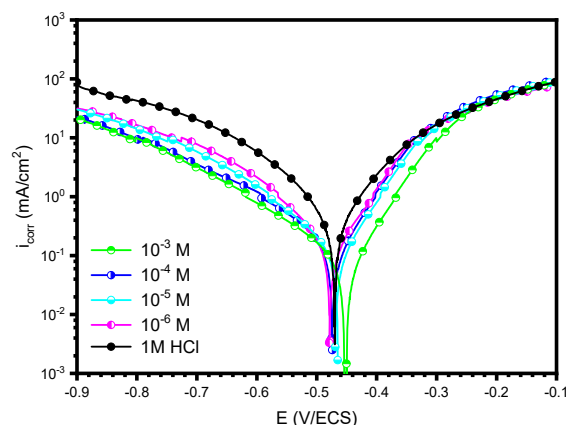


**Figure 3.** PDP curves for MS in 1 M HCl medium, both unprotected and protected, by varying concentrations of studied epoxy resin.

**Table 1.** PDP parameters for MS in 1 M HCl solution, both unprotected and protected, by varying concentrations of TGP.

	Con. (M)	$-E_{corr}$ (mV/SCE)	$i_{corr}$ ( $\mu\text{A cm}^{-2}$ )	$-\beta_c$ ( $\text{mV dec}^{-1}$ )	Ba ( $\text{mV dec}^{-1}$ )	$\eta_{PDP}$ (%)
HCl	1	498	983.0	92.0	104.0	-
TGP	$10^{-6}$	477	227.24	185.5	113.5	76.88
	$10^{-5}$	473	192.30	117.3	91.2	80.43
	$10^{-4}$	464	154.1	141.1	89.8	84.24
	$10^{-3}$	453	147.42	194.3	151.2	85.0

### 3.4. EIS Analysis

To understand and evaluate the corrosion inhibition of MS electrode surfaces, the elaborated epoxy prepolymer was used and investigated. Figure 4 displays the Nyquist curves for the anticorrosion protection property of the epoxy prepolymer inhibitor in an acidic solution, both unprotected and protected, with varying concentrations of the studied inhibitor. Additionally, careful examination of the Nyquist curves suggests that the corrosion inhibition mechanism was the same for the unprotected and protected experiments owing to the semicircle loops [7,33]. As indicated in Figure 4, judging from the significant increases in the sizes of the semicircles and the charge transfer resistance in the different concentrations of epoxy prepolymer, one could conclude that the TGP synthesized was able to adsorb on the metallic substrates, forming a barrier and restricting the metal dissolution [34,35]. Then, EIS results were subsequently fitted from an equivalent circuit comprising the constant phase element (CPE), the solution resistance ( $R_s$ ) and the charge transfer resistance ( $R_{ct}$ ), as displayed in Figure 4. The EIS parameters are listed in Table 2, and the analysis of the results reflected an important increase in the values of charge transfer resistance from 34.81 to 210.2  $\Omega \text{ cm}^2$  for 1 M HCl alone and with the  $10^{-3}$  M of TGP epoxy prepolymer, respectively, showing the highest charge transfer resistance through the tested inhibitor at the MS/electrolyte interface [17]. In addition, the highest charge transfer resistance values, as shown in Table 2, confirmed the inhibitory efficiency of the epoxy prepolymer in the corrosion inhibition of metallic surfaces in 1 M HCl solution. Furthermore, the phase element constant values are revealed in the different concentrations of epoxy prepolymer in the 1 M HCl solution, resulting in the formation of a covering layer on the MS surface through epoxy prepolymer, and the increases in the thickness of protective layer as more  $\text{H}_2\text{O}$  molecules were replaced by the epoxy prepolymer at highest concentrations [36–38]. As seen in Table 2, the  $n_{dl}$  values were investigated to classify the CPE as well as revealing the nature of the metallic substrates' electrode area. According to data displayed in Table 2, the  $n_{dl}$  values of both the unprotected and protected MS by different concentrations of epoxy prepolymer appeared to be lower and close to 1, suggesting the pseudocapacitive nature of the CPE. These results indicate that the TGP epoxy prepolymer is a good inhibitor compared to other macromolecules used as corrosion inhibitors [39,40].

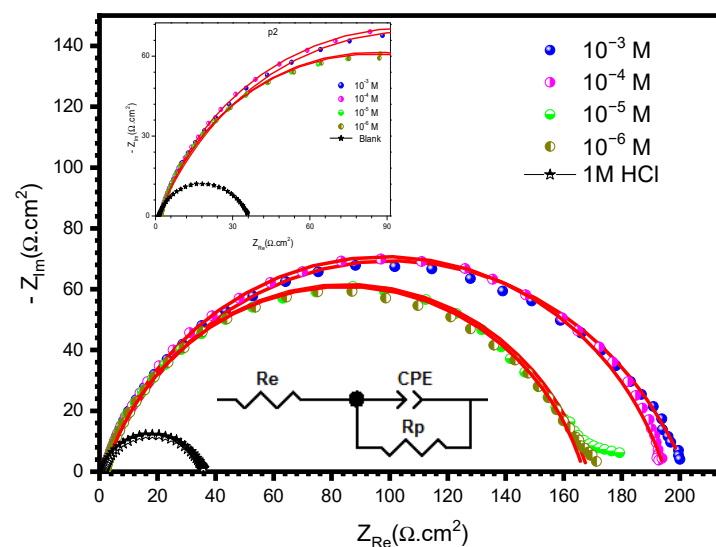


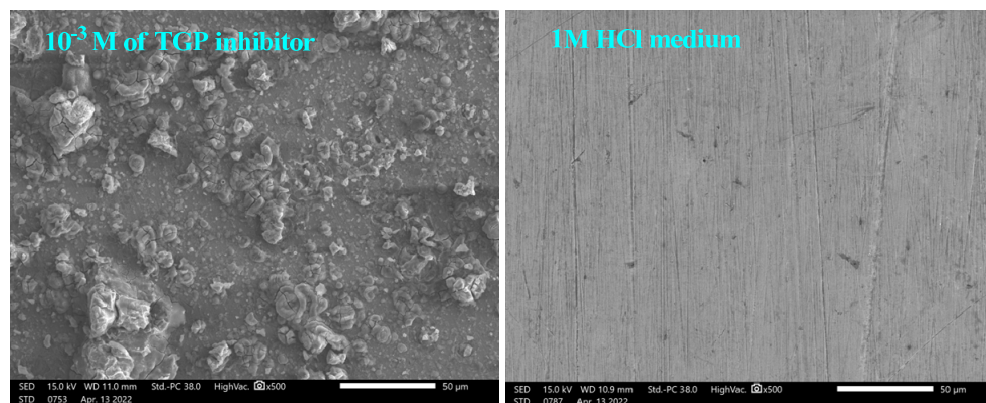
**Figure 4.** Nyquist curves for MS plunged in 1 M HCl medium, both unprotected and protected by varying concentrations of TGP.

**Table 2.** EIS parameters for MS plunged in 1 M HCl solution, both unprotected and protected by varying concentrations of TGP.

	Concentrations (M)	$R_s$ ( $\Omega \text{ cm}^2$ )	$R_{ct}$ ( $\Omega \text{ cm}^2$ )	$Q$ ( $\mu\text{F s}^{n-1}$ )	$n_{dl}$	$C_{dl}$ ( $\mu\text{F/cm}^2$ )	$\eta_{EIS}$ (%)
HCl	1	1.107	34.81	420.0	0.772	121.0	-
TGP	$10^{-6}$	1.903	165.9	183.4	0.810	74.31	79.01
	$10^{-5}$	1.622	166.5	180.9	0.808	73.00	79.09
	$10^{-4}$	1.930	194.5	149.7	0.804	63.00	82.14
	$10^{-3}$	2.271	210.2	133.1	0.798	54.33	87.17

### 3.5. SEM/EDS Characterization

To know and understand the adsorption mechanism between the MS electrode surface and the synthesized inhibitory prepolymer, SEM and EDS techniques were investigated and discussed. Figure 5 illustrates the SEM images of the MS electrode plunged in 1 M HCl solution for unprotected (a) and protected by lower concentration ( $10^{-3}$  M) of used inhibitory resin (b). In fact, SEM images show that the surface of the MS electrode had become rough due to the deposition of a protective layer [22]. Figure 6 illustrates the X-ray energy dispersive spectroscopy (EDS) analysis of the MS surface, for both unprotected and that protected with a lower concentration of the used inhibitor, in 1 M HCl medium. According to the results displayed in Figure 6, it can be seen that the iron content of the MS surface increases from 66.03 to 66.16%, and the Cr, Mn, Ni and Mo elemental peaks disappear with added TGP inhibitory prepolymer at a lower concentration. Furthermore, elemental oxygen content peaks appeared, and the carbon content increased in the presence of  $10^{-3}$  M of the studied inhibitor due to the oxygen heteroatoms and carbon present in the molecule of TGP prepolymer synthesized, resulting in the inhibitory resin reducing the density of active centers on the MS area by forming the protective layer and retarding corrosion inhibition [40].

**Figure 5.** SEM images for MS surface plunged in 1 M HCl medium for both unprotected and protected by  $10^{-3}$  M of TGP.

### 3.6. Contact Angle Characterization

The layer that forms on the MS electrode surface and its hydrophilic or hydrophobic characteristics can be understood through contact angle analysis of MS surfaces that are both unprotected and protected by  $10^{-3}$  M of TGP prepolymer after being in contact with a 1 M HCl solution (Figure 7). The unprotected MS area in diiodomethane, water and formamide had contact angles of 12.5, 30.2 and 19.6°, respectively. These data can be explained by the hydrophilicity characteristic (favors water). The formation of some polar inorganic corrosion products is responsible for the hydrophilic phenomena. However, the contact angles of the MS surface protected by  $10^{-3}$  M of TGP in diiodomethane, water and

formamide were 65.4, 89.9 and 62°, respectively. These data indicate that the MS surface protected by  $10^{-3}$  M of TGP has a hydrophobic character (does not favor water). This result confirms the formation of a hydrophobic layer on the MS electrode area. By comparing between the unprotected MS and that protected by  $10^{-3}$  M of TGP, we can conclude that the MS electrode surface protected with  $10^{-3}$  M of TGP inhibitor has a more hydrophobic character than the unprotected MS, leading to more prevention of corrosion attacking the steel surface. Additionally, the total energy of the MS surfaces, both unprotected and that protected with  $10^{-3}$  M of TGP, was 54.7 and 28.6 mJ/m<sup>2</sup>, respectively. The results in Figure 7 confirm that a hydrophilic layer has formed on the MS area [22].

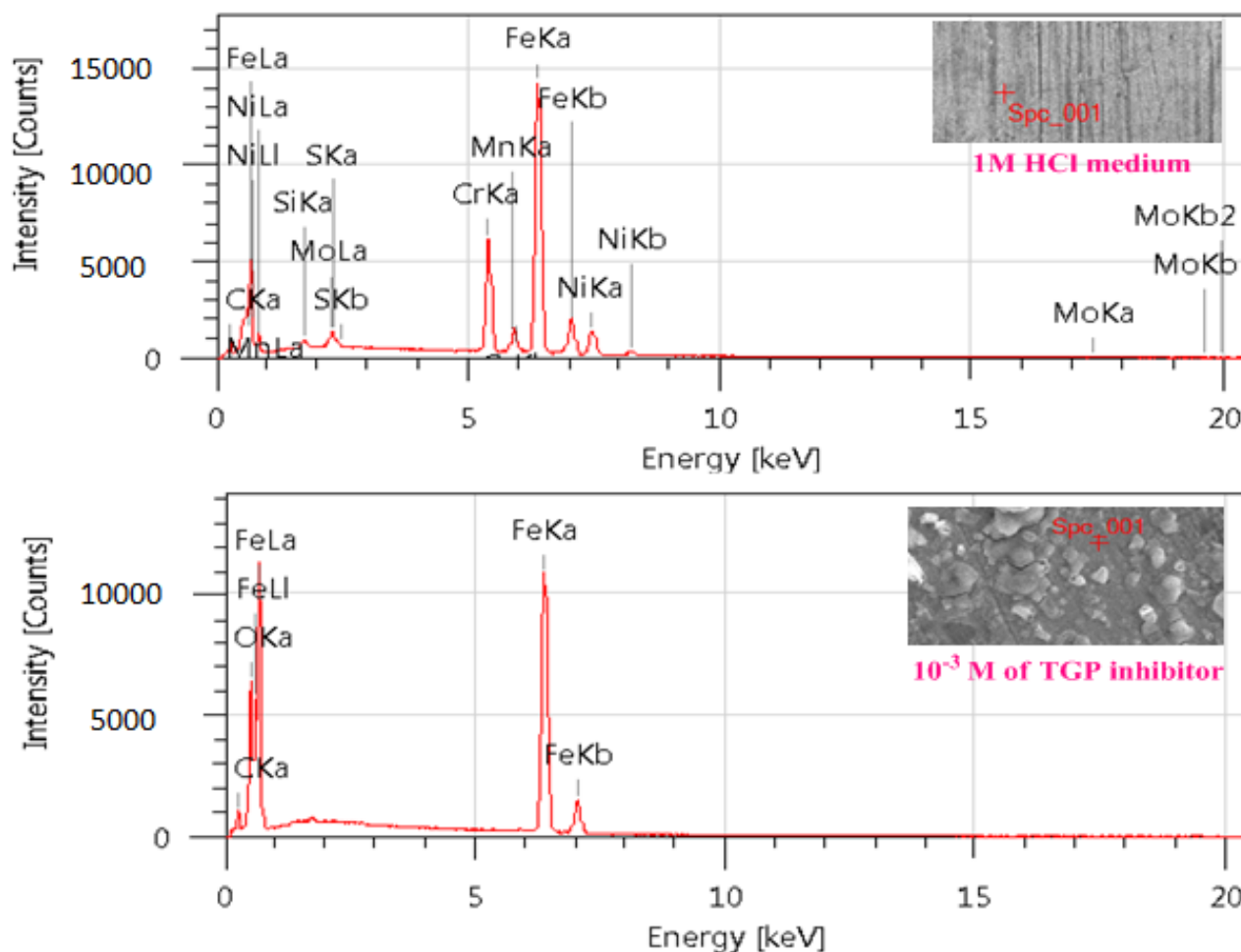


**Figure 6.** EDS spectra for MS electrode after immersion in 1 M HCl medium for both unprotected and protected by  $10^{-3}$  M of TGP.

### 3.7. Adsorption Study

To know the adsorption mechanism between the TGP epoxy prepolymer and a mild steel electrode surface in 1 M HCl medium, experimental results obtained from both PDP and EIS measurements were calculated using the various adsorption isotherm equations and the best fit, which, in this case, was the Langmuir adsorption isotherm model, as shown in Figure 8. The results from PDP and EIS analysis indicate that the TGP prepolymer synthesized was adsorbed on the metallic substrates by forming a protective layer that protects the mild steel against corrosion [40]. The obtained parameters from the studied Langmuir adsorption for the inhibitory resin are illustrated in Table 3. According to the results obtained from the two techniques (PDP and EIS), the coefficient values ( $R^2$ ) are 1 and 0.9999 for PDP and EIS, respectively, which conformed well to the Langmuir adsorption isotherm. These results show that the inhibitory prepolymer can be adsorbed on the mild

steel area according to the best model that can be used to interpret this particular phenomenon. Adsorption Gibbs energy variation values ( $\Delta G_{ads}$ ) give more information about the adsorption mode of the inhibitor and the MS area. Additionally, the  $\Delta G_{ads}$  values were higher than  $-40 \text{ kJ mol}^{-1}$  and less than  $-20 \text{ kJ mol}^{-1}$ , indicating the chemisorption and physisorption modes, respectively [22]. The Langmuir adsorption isotherm model and the adsorption Gibbs energy variation could be calculated according to Equations (3) and (4):

$$\frac{C_{inh}}{\theta} = \frac{1}{K_{ads}} + C_{inh} \tag{3}$$

$$\Delta G_{ads}^{\circ} = -R \times T \times \ln(55.5 \times K_{ads}) \tag{4}$$

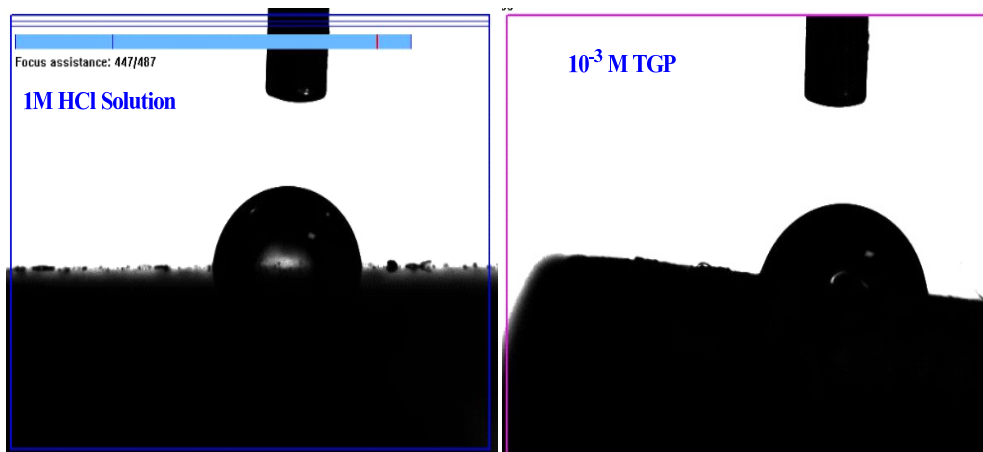


Figure 7. CA analysis of MS after immersion in 1 M HCl solution, both unprotected and protected by  $10^{-3} \text{ M}$  of TGP.

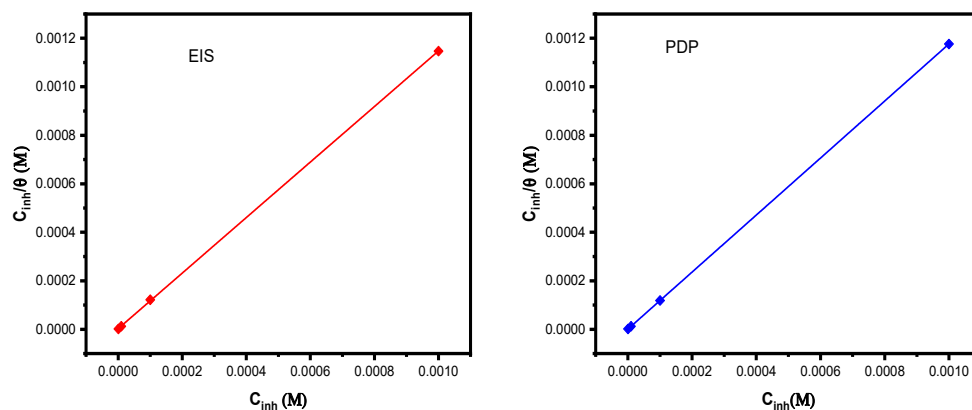


Figure 8. Langmuir adsorption isotherm model of TGP for MS in 1 M HCl medium using two techniques (PDP and EIS) at 298 K.

Table 3. Adsorption and thermodynamic parameters for the corrosion of mild steel in the presence of the TGP at 303 k in acidic media.

TGP	Techniques	R <sup>2</sup>	Slopes	Intercept (10 <sup>-6</sup> )	K <sub>ads</sub> (M <sup>-1</sup> )	ΔG <sub>ads</sub> (KJ mol <sup>-1</sup> )
	PDP	1	1.1759	0.622719	3.87	-42.13
	EIS	0.9999	1.14491	2.71049	1.95	-43.74

$C_{inh}$ ,  $\theta$ ,  $K_{ads}$ ,  $R$  and  $T$  are the inhibitory concentration, the surface coverage degree, the adsorption equilibrium constant, the perfect gas constant and the used temperature, respectively.

As the data displayed in Table 3 show, the  $\Delta G_{ads}$  values for PDP and EIS analyses were 42.13 and 43.74, respectively, suggesting that the epoxy prepolymer inhibitory adsorbed on the MS area by chemisorption mode. Furthermore, the chemisorption model of the TGP prepolymer could be due to the bond types between iron ions and the bond double of carbonyl compound (C=O) and free electron pairs of oxygen heteroatoms present in the synthesized prepolymer.

### 3.8. Temperature Effect and Thermodynamic Parameters

From the experimental data (PDP and EIS measurements), it was established that the used inhibitory epoxy resin was adsorbed on the MS area by forming a protective layer that protects the metal against corrosion. So, the inhibitory efficiency needs to be used and investigated at different temperatures (298, 308, 318 and 328 K) using the PDP technique. Figure 9 illustrates the PDP plots for the MS electrode both unprotected and protected by  $10^{-3}$  M of the studied inhibitor. As the data illustrate in Table 4, the corrosion current density of the MS electrode, both unprotected and protected by  $10^{-3}$  M, increases with increasing temperatures and its inhibitory efficiency decreased, showing that the increases in temperature accelerated the corrosion of the MS surface in the 1 M HCl medium, and it was found that the inhibitory efficiency of the MS electrode in 1 M HCl solution after adding the lowest concentration decreases from 85 to 81.62% for 298 and 328 K, respectively [22]. This behavior can be explained by the weakening bond of the inhibitory TGP prepolymer, resulting in a reduction in the coverage surface and its inhibitory efficiency decreasing.

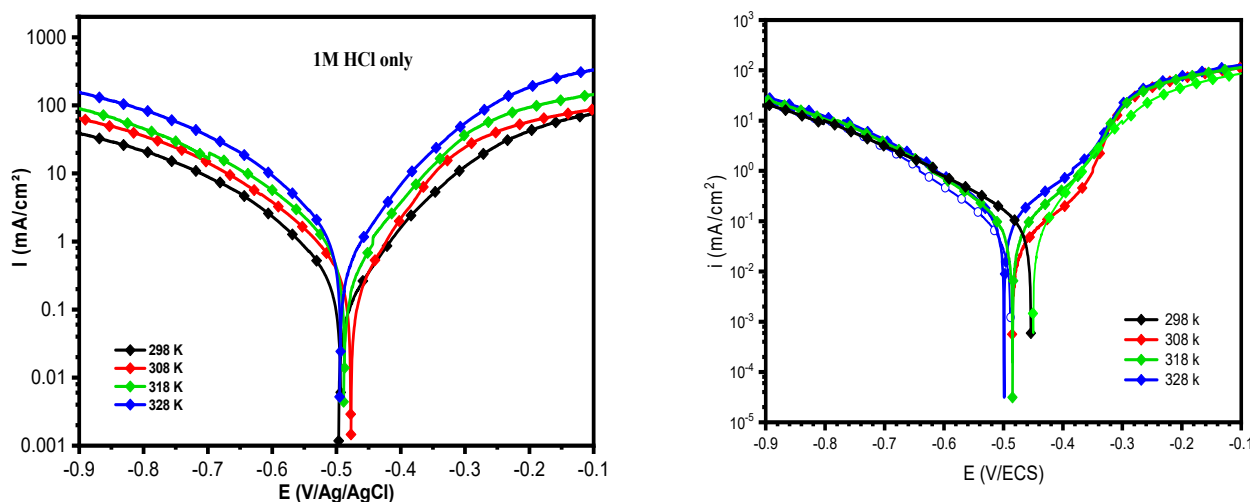


Figure 9. PDP curves of MS electrode in 1 M HCl solution, both unprotected and protected with  $10^{-3}$  M of TGP at varying temperatures.

Table 4. PDP and thermodynamic parameters of MS in 1 M HCl medium, both unprotected and protected with  $10^{-3}$  M of TGP at 298, 308, 318 and 328 K.

T K	$-E_{corr}$ mV <sub>Ag/AgCl</sub>	$i_{corr}$ $\mu A\ cm^{-2}$	$-\beta_c$ mV dec <sup>-1</sup>	$\eta_{PC}$ %	$E_a$ kJ mol <sup>-1</sup>	$\Delta H_a$ kJ mol <sup>-1</sup>	$-\Delta S_a$ J mol <sup>-1</sup> K <sup>-1</sup>
MS electrode/1 M HCl solution							
298	498	983	92	-	21.0	18.5	126.0
308	491	1200	184	-			
318	475	1450	171	-			
328	465	2200	161	-			
Inhibitory resin/MS electrode/1 M HCl solution							
298	453	147.42	194.3	85.0	26.53	23.14	123.37
308	486	798.0	157.2	83.5			
318	494	255.0	167.1	82.2			
328	499	404.19	171.4	81.6			

The Arrhenius model was used to determine the activation energy of the MS electrode surface according to Equation (5). Additionally, the enthalpy and entropy activation were calculated by the following Equation (6):

$$i_{\text{corr}} = A \exp\left(-\frac{E_a}{RT}\right) \quad (5)$$

$$i_{\text{corr}} = \frac{RT}{hN} \exp\left(\frac{\Delta S_a}{T}\right) \exp\left(-\frac{\Delta H_a}{RT}\right) \quad (6)$$

$N$ ,  $T$ ,  $E_a$ ,  $R$ ,  $h$ ,  $K$ ,  $\Delta H_a$  and  $\Delta S_a$  are Avogadro's number, the absolute temperature, the activation energy, the perfect gas constant, Planck's constant, the pre-exponential factor, the activation enthalpy and the activation entropy, respectively.

Figure 10 illustrates the  $\text{Log}(i_{\text{corr}})$  as a function of  $1000/T$  and  $\text{Log}(i_{\text{corr}}/T)$  as a function of  $1000/T$  curves. As the data display in Table 4,  $E_a$  reflects the minimum energy required for an effective collision between inhibitory resin and MS surface. According to the results listed in Table 4, the  $E_a$  value significantly increases, indicating that the corrosion of the MS surface increases in the presence of the inhibitory resin due to the TGP prepolymer being adsorbed on the metallic surface, which occupies the active centers of the reaction and inhibits the corrosion reaction. Furthermore, the activation energy of the synthesized resin is higher than that of the 1 M HCl alone, reflecting that the investigated molecule has good anticorrosive protection. Furthermore, the activation enthalpy positively indicates that the dissolution of the MS surface added to corrosion inhibition is a heat absorption process. The activation entropy negatively indicates the activation complex is an interaction phase and not a dissociation phase in the rate-determining phase. According to the presented data in Table 4, with the inhibitory prepolymer, the  $\Delta S_a$  value is higher than that of the 1 M HCl only, resulting in the formation of a protective layer on the MS surface.

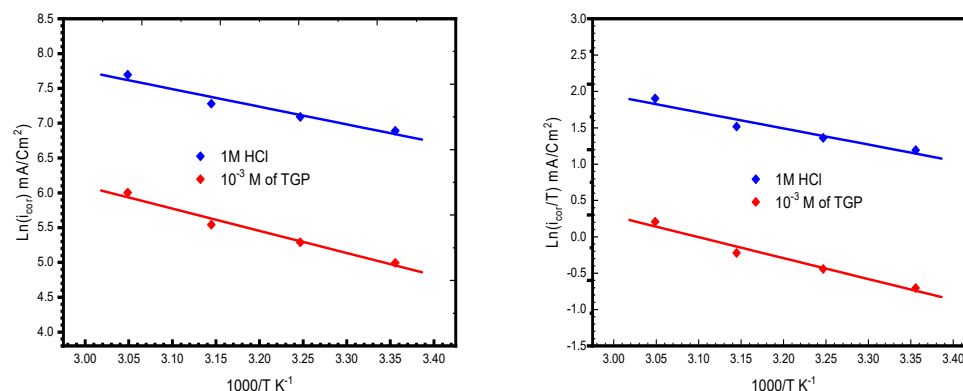


**Figure 10.**  $\text{Ln}(i_{\text{corr}})$  as function of  $1000/T$  (left) and  $\text{Ln}(i_{\text{corr}}/T)$  as function of  $1000/T$  (right) curves for MS in 1 M HCl solution, both unprotected and protected by  $10^{-3}$  M of TGP.

#### 4. Conclusions

The corrosion inhibition of a tetrafunctional epoxy prepolymer (TGP) has been studied via electrochemical measurements, surface analyses and calculation studies. The results from the PDP data suggest that the TGP adsorbed strongly onto the MS surface, behaving as a mixed-type corrosion inhibitor. The Langmuir adsorption isotherm and slope indicate monolayer adsorption with  $R^2$  value approaching unity. PDP and EIS have high inhibitory efficiencies at lower concentration of the TGP. The Gibbs free energy values for the adsorption of the TGP prepolymer indicates chemisorption. SEM and EDS analysis reveal the potential ability of TGP in the 1 M HCl solution. Additionally, the adsorption isotherm obeys the Langmuir model.

**Author Contributions:** Investigation, writing—original draft preparation, review and editing, R.H.; formal analysis, R.L., A.E.M., S.E. and M.G.; supervision, M.E.T. and M.R. H.R.V. editing. All authors have read and agreed to the published version of the manuscript.

**Funding:** This research received no external funding.

**Institutional Review Board Statement:** Not applicable.

**Informed Consent Statement:** Not applicable.

**Data Availability Statement:** The data that support the findings of this study are available from the corresponding author upon reasonable request.

**Acknowledgments:** We would like to thank Anouar El Magri and Hamid Reza Vanei for their support. Also, I would like to thank to all authors.

**Conflicts of Interest:** The authors declare no conflict of interest.

## References

1. Rbaa, M.; Benhiba, F.; Hsissou, R.; Lakhrissi, Y.; Lakhrissi, B.; Touhami, M.E.; Warad, I.; Zarrouk, A. Green synthesis of novel carbohydrate polymer chitosan oligosaccharide grafted on d-glucose derivative as bio-based corrosion inhibitor. *J. Mol. Liq.* **2021**, *322*, 114549. [\[CrossRef\]](#)
2. Galai, M.; Rbaa, M.; Ouakki, M.; Abousalem, A.S.; Ech-Chihbi, E.; Dahmani, K.; Dkhireche, N.; Lakhrissi, B.; EbnTouhami, M. Chemically functionalized of 8-hydroxyquinoline derivatives as efficient corrosion inhibition for steel in 1.0 M HCl solution: Experimental and theoretical studies. *Surf. Interfaces* **2020**, *21*, 100695. [\[CrossRef\]](#)
3. Benhiba, F.; Hsissou, R.; Benzekri, Z.; Belghiti, M.E.; Lamhamdi, A.; Bellaouchou, A.; Guenbour, A.; Boukhris, S.; Oudda, H.; Warad, I.; et al. Nitro substituent effect on the electronic behavior and inhibitory performance of two quinoxaline derivatives in relation to the corrosion of mild steel in 1 M HCl. *J. Mol. Liq.* **2020**, *312*, 113367. [\[CrossRef\]](#)
4. Benhiba, F.; Hsissou, R.; Benzekri, Z.; Echihi, S.; El-Blilak, J.; Boukhris, S.; Bellaouchou, A.; Guenbour, A.; Oudda, H.; Warad, I.; et al. DFT/electronic scale, MD simulation and evaluation of 6-methyl-2-(p-tolyl)-1,4-dihydroquinoxaline as a potential corrosion inhibition. *J. Mol. Liq.* **2021**, *335*, 116539. [\[CrossRef\]](#)
5. Lachiri, A.; El Faydy, M.; Benhiba, F.; Zarrok, H.; El Azzouzi, M.; Zertoubi, M.; Azzi, M.; Lakhrissi, B.; Zarrouk, A. Inhibitor effect of new azomethine derivative containing an 8-hydroxyquinoline moiety on corrosion behavior of mild carbon steel in acidic media. *Int. J. Corros. Scale Inhib.* **2018**, *7*, 609–632.
6. Damej, M.; Hsissou, R.; Berisha, A.; Azgaou, K.; Sadiku, M.; Benmessaoud, M.; Labjar, N.; El hajjaji, S. New epoxy resin as a corrosion inhibitor for the protection of carbon steel C38 in 1 M HCl. experimental and theoretical studies (DFT, MC, and MD). *J. Mol. Struct.* **2022**, *1254*, 132425. [\[CrossRef\]](#)
7. Dagdag, O.; Safi, Z.; Hsissou, R.; Erramli, H.; El Bouchti, M.; Wazzan, N.; Guo, L.; Verma, C.; Ebenso, E.; El Harfi, A. Epoxy pre-polymers as new and effective materials for corrosion inhibition of carbon steel in acidic medium: Computational and experimental studies. *Sci. Rep.* **2019**, *9*, 11715. [\[CrossRef\]](#)
8. Dagdag, O.; Hsissou, R.; El Harfi, A.; El Gana, L.; Safi, Z.; Guo, L.; Verma, C.; Ebenso, E.E.; El Gouri, M. Development and Anti-corrosion Performance of Polymeric Epoxy Resin and their Zinc Phosphate Composite on 15CDV6 Steel in 3wt% NaCl: Experimental and Computational Studies. *J. Bio-Tribo-Corros.* **2020**, *6*, 112. [\[CrossRef\]](#)
9. Verma, C.; Olasunkanmi, L.O.; Akpan, E.D.; Quraishi, M.A.; Dagdag, O.; El Gouri, M.; Sherif, E.-S.M.; Ebenso, E.E. Epoxy resins as anticorrosive polymeric materials: A review. *React. Funct. Polym.* **2020**, *156*, 104741. [\[CrossRef\]](#)
10. Hsissou, R.; Benzidia, B.; Hajjaji, N.; Elharfi, A. Elaboration, Electrochemical Investigation and morphological Study of the Coating Behavior of a new Polymeric Polyepoxide Architecture: Crosslinked and Hybrid Decaglycidyl of Phosphorus Penta methylene Dianiline on E24 Carbon Steel in 3.5% NaCl. *Port. Electrochim. Acta* **2019**, *37*, 179–191. [\[CrossRef\]](#)
11. Hsissou, R.; Benzidia, B.; Rehioui, M.; Berradi, M.; Berisha, A.; Assouag, M.; Hajjaji, N.; Elharfi, A. Anticorrosive property of hexafunctional epoxy polymer HGTMDAE for E24 carbon steel corrosion in 1.0 M HCl: Gravimetric, electrochemical, surface morphology and molecular dynamic simulations. *Polym. Bull.* **2020**, *77*, 3577–3601. [\[CrossRef\]](#)
12. Hsissou, R.; Bekhta, A.; Elharfi, A.; Benzidia, B.; Hajjaji, N. Theoretical and electrochemical studies of the coating behavior of a new epoxy polymer: Hexaglycidyl ethylene of methylene dianiline (HGEMDA) on E24 steel in 3.5% NaCl. *Port. Electrochim. Acta* **2018**, *36*, 101–117. [\[CrossRef\]](#)
13. Yuan, W.; Hu, Q.; Zhang, J.; Huang, F.; Liu, J. Hydrophobic Modification of Graphene Oxide and Its Effect on the Corrosion Resistance of Silicone-Modified Epoxy Resin. *Metals* **2021**, *11*, 89. [\[CrossRef\]](#)
14. Xiong, G.; Kang, P.; Zhang, J.; Li, B.; Yang, J.; Chen, G.; Zhou, Z.; Li, Q. Improved adhesion, heat resistance, anticorrosion properties of epoxy resins/POSS/methyl phenyl silicone coatings. *Prog. Org. Coat.* **2019**, *135*, 454–464. [\[CrossRef\]](#)
15. Hsissou, R.; About, S.; Benhiba, F.; Seghiri, R.; Safi, Z.; Kaya, S.; Briche, S.; Serdaroglu, G.; Erramli, H.; Elbachiri, A.; et al. Insight into the corrosion inhibition of novel macromolecular epoxy resin as highly efficient inhibitor for carbon steel in acidic mediums: Synthesis, characterization, electrochemical techniques, AFM/UV-Visible and computational investigations. *J. Mol. Liq.* **2021**, *337*, 116492. [\[CrossRef\]](#)

16. Hsissou, R.; About, S.; Safi, Z.; Benhiba, F.; Wazzan, N.; Guo, L.; Nouneh, K.; Briche, S.; Erramli, H.; Touhami, M.E.; et al. Synthesis and anticorrosive properties of epoxy polymer for CS in [1 M] HCl solution: Electrochemical, AFM, DFT and MD simulations. *Constr. Build. Mater.* **2021**, *270*, 121454. [[CrossRef](#)]
17. El-Aouni, N.; Hsissou, R.; Safi, Z.; About, S.; Benhiba, F.; El Azzaoui, J.; Haldhar, R.; Wazzan, N.; Guo, L.; Erramli, H.; et al. Performance of two new epoxy resins as potential corrosion inhibitors for carbon steel in 1MHCl medium: Combining experimental and computational approaches. *Colloids Surf. A Physicochem. Eng. Asp.* **2021**, *626*, 127066. [[CrossRef](#)]
18. Molhi, A.; Hsissou, R.; Damej, M.; Berisha, A.; Thaçi, V.; Belafhaili, A.; Benmessaoud, M.; Labjar, N.; El Hajjaji, S. Contribution to the corrosion inhibition of C38 steel in 1 M hydrochloric acid medium by a new epoxy resin PGEPPP. *Int. J. Corros. Scale Inhib* **2021**, *10*, 399–418.
19. Molhi, A.; Hsissou, R.; Damej, M.; Berisha, A.; Bamaarouf, M. Performance of two epoxy resins against corrosion of C38 steel in 1 M HCl: Electrochemical, thermodynamic and theoretical assessment. *Int. J. Corros. Scale Inhib.* **2021**, *10*, 812–837.
20. About, S.; Hsissou, R.; Erramli, H.; Chebabe, D.; Salim, R.; Kaya, S.; Hajjaji, N. Gravimetric, electrochemical and theoretical study, and surface analysis of novel epoxy resin as corrosion inhibitor of carbon steel in 0.5 M H<sub>2</sub>SO<sub>4</sub> solution. *J. Mol. Struct.* **2021**, *1245*, 131014. [[CrossRef](#)]
21. About, S.; Hsissou, R.; Chebabe, D.; Erramli, H.; Hajjaji, N. Investigation of the anti-corrosion properties of Galactomannan as additive in epoxy coatings for carbon steel: Rheological and electrochemical study. *Inorg. Chem. Commun.* **2021**, *134*, 108971. [[CrossRef](#)]
22. Hsissou, R.; Azogagh, M.; Benhiba, F.; Echihi, S.; Galai, M.; Shaim, A.; Bahaj, H.; Briche, S.; Kaya, S.; Serdaroğlu, G.; et al. Insight of development of two cured epoxy polymer composite coatings as highly protective efficiency for carbon steel in sodium chloride solution: DFT, RDE, FFV and MD approaches. *J. Mol. Liq.* **2022**, *360*, 119406. [[CrossRef](#)]
23. Guo, L.; Safi, Z.S.; Kaya, S.; Shi, W.; Tüzün, B.; Altunay, N.; Kaya, C. Anticorrosive Effects of Some Thiophene Derivatives Against the Corrosion of Iron: A Computational Study. *Front. Chem.* **2018**, *6*, 155. [[CrossRef](#)] [[PubMed](#)]
24. Erdoğan, Ş.; Safi, Z.S.; Kaya, S.; Işın, D.Ö.; Guo, L.; Kaya, C. A computational study on corrosion inhibition performances of novel quinoline derivatives against the corrosion of iron. *J. Mol. Struct.* **2017**, *1134*, 751–761. [[CrossRef](#)]
25. Dagdag, O.; Hsissou, R.; El Harfi, A.; Safi, Z.; Berisha, A.; Verma, C.; Ebenso, E.E.; Quraishi, M.A.; Wazzan, N.; Jodeh, S.; et al. Epoxy resins and their zinc composites as novel anti-corrosive materials for copper in 3% sodium chloride solution: Experimental and computational studies. *J. Mol. Liq.* **2020**, *315*, 113757. [[CrossRef](#)]
26. Hsissou, R.; Dagdag, O.; Berradi, M.; El Bouchti, M.; Assouag, M.; El Bachiri, A.; Elharfi, A. Investigation of structure and rheological behavior of a new epoxy polymer pentaglycidyl ether pentabispheol A of phosphorus and of its composite with natural phosphate. *SN Appl. Sci.* **2019**, *1*, 869. [[CrossRef](#)]
27. Hsissou, R.; Berradi, M.; El Bouchti, M.; El Bachiri, A.; El Harfi, A. Synthesis characterization rheological and morphological study of a new epoxy resin pentaglycidyl ether pentaphenoxy of phosphorus and their composite (PGEPPP/MDA/PN). *Polym. Bull.* **2019**, *76*, 4859–4878. [[CrossRef](#)]
28. Benhiba, F.; Benzekri, Z.; Guenbour, A.; Tabyaoui, M.; Bellaouchou, A.; Boukhris, S.; Oudda, H.; Warad, I.; Zarrouk, A. Combined electronic/atomic level computational, surface (SEM/EDS), chemical and electrochemical studies of the mild steel surface by quinoxalines derivatives anti-corrosion properties in 1 mol·L<sup>-1</sup> HCl solution. *Chin. J. Chem. Eng.* **2020**, *28*, 1436–1458. [[CrossRef](#)]
29. Hsissou, R.; Benhiba, F.; About, S.; Dagdag, O.; Benkhaya, S.; Berisha, A.; Erramli, H.; Elharfi, A. Trifunctional epoxy polymer as corrosion inhibition material for carbon steel in 1.0 M HCl: MD simulations, DFT and complexation computations. *Inorg. Chem. Commun.* **2020**, *115*, 107858. [[CrossRef](#)]
30. Hsissou, R.; Benhiba, F.; Dagdag, O.; El Bouchti, M.; Nouneh, K.; Assouag, M.; Briche, S.; Zarrouk, A.; Elharfi, A. Development and potential performance of prepolymer in corrosion inhibition for carbon steel in 1.0 M HCl: Outlooks from experimental and computational investigations. *J. Colloid Interface Sci.* **2020**, *574*, 43–60. [[CrossRef](#)] [[PubMed](#)]
31. Echihi, S.; Hsissou, R.; Benzbiria, N.; Afrokh, M.; Boudalia, M.; Bellaouchou, A.; Guenbour, A.; Azzi, M.; Tabyaoui, M. Performance of Methanolic Extract of Artemisia herba alba as a Potential Green Inhibitor on Corrosion Behavior of Mild Steel in Hydrochloric Acid Solution. *Biointerface Res. Appl. Chem.* **2021**, *11*, 14751–14763.
32. Dagdag, O.; Hsissou, R.; Berisha, A.; Erramli, H.; Hamed, O.; Jodeh, S.; El Harfi, A. Polymeric-based epoxy cured with a polyaminoamide as an anticorrosive coating for aluminum 2024-T3 surface: Experimental studies supported by computational modeling. *J. Bio-Tribo-Corros.* **2019**, *5*, 58. [[CrossRef](#)]
33. Hsissou, R.; Dagdag, O.; Berradi, M.; El Bouchti, M.; Assouag, M.; Elharfi, A. Development rheological and anti-corrosion property of epoxy polymer and its composite. *Heliyon* **2019**, *5*, e02789. [[CrossRef](#)] [[PubMed](#)]
34. Hsissou, R.; Dagdag, O.; About, S.; Benhiba, F.; Berradi, M.; El Bouchti, M.; Berisha, A.; Hajjaji, N.; Elharfi, A. Novel derivative epoxy resin TGETET as a corrosion inhibition of E24 carbon steel in 1.0 M HCl solution. Experimental and computational (DFT and MD simulations) methods. *J. Mol. Liq.* **2019**, *284*, 182–192. [[CrossRef](#)]
35. Ouass, A.; Galai, M.; Ouakki, M.; Ech-Chihbi, E.; Kadiri, L.; Hsissou, R.; Essaadaoui, Y.; Berisha, A.; Cherkaoui, M.; Lebki, A.; et al. Poly(sodium acrylate) and Poly(acrylic acid sodium) as an eco-friendly corrosion inhibitor of mild steel in normal hydrochloric acid: Experimental, spectroscopic and theoretical approach. *J. Appl. Electrochem.* **2021**, *51*, 1009–1032. [[CrossRef](#)]

36. Hsissou, R.; Benhiba, F.; Echihi, S.; Benzidia, B.; Cherrouf, S.; Haldhar, R.; Alvi, P.A.; Kaya, S.; Serdaroglu, G.; Zarrouk, A. Performance of curing epoxy resin as potential anticorrosive coating for carbon steel in 3.5% NaCl medium: Combining experimental and computational approaches. *Chem. Phys. Lett.* **2021**, *783*, 139081. [[CrossRef](#)]
37. Hsissou, R.; Benhiba, F.; Echihi, S.; Benkhaya, S.; Hilali, M.; Berisha, A.; Briche, S.; Zarrouk, A.; Nouneh, K.; Elharfi, A. New epoxy composite polymers as a potential anticorrosive coatings for carbon steel in 3.5% NaCl solution: Experimental and computational approaches. *Chem. Data Collect.* **2021**, *31*, 100619. [[CrossRef](#)]
38. Abd-El-Nabey, B.; Abdel-Gaber, A.; Elewady, G.; Sadeek, M.; Abd-El-Rhman, H. Inhibitive action of benzaldehyde thiosemicarbazones on the corrosion of mild steel in 3 MH<sub>3</sub>PO<sub>4</sub>. *Int. J. Electrochem. Sci* **2012**, *7*, 11718–11733.
39. Abdallah, M.; Zaafarany, I.; Fouda, A.; El-Kader, A. Inhibition of zinc corrosion by some benzaldehyde derivatives in HCl solution. *J. Mater. Eng. Perform.* **2012**, *21*, 995–1002. [[CrossRef](#)]
40. Hsissou, R.; About, S.; Seghiri, R.; Rehioui, M.; Berisha, A.; Erramli, H.; Assouag, M.; Elharfi, A. Evaluation of corrosion inhibition performance of phosphorus polymer for carbon steel in [1 M] HCl: Computational studies (DFT, MC and MD simulations). *J. Mater. Res. Technol.* **2020**, *9*, 2691–2703. [[CrossRef](#)]